

Experimental research on seismic behavior of SRC-RC transfer columns

Kai Wu ^{*1}, Jianyang Xue ^{2a}, Yang Nan ^{1b} and Hongtie Zhao ^{2c}

¹ College of Civil and Transportation Engineering, Hohai University, Nanjing 210098, China

² School of Civil Engineering, Xi'an University of Architecture & Technology, Xi'an 710055, China

(Received April 25, 2015, Revised February 28, 2016, Accepted March 09, 2016)

Abstract. It was found that the lateral stiffness changes obvious at the transfer position of the section configuration from SRC to RC. This particular behavior leads to that the transfer columns become as the important elements in SRC-RC hybrid structures. A comprehensive study was conducted to investigate the seismic behavior of SRC-RC transfer columns based on a low cyclic loading test of 16 transfer columns compared with 1 RC column. Test results shows three failure modes for transfer columns, which are shear failure, bond failure and bend failure. Its seismic behavior was completely analyzed about the failure mode, hysteretic and skeleton curves, bearing capacity deformation ability, stiffness degradation and energy dissipation. It is further determined that displacement ductility coefficient of transfer columns changes from 1.97 to 5.99. The stiffness of transfer columns are at the interval of SRC and RC, and hence transfer columns can play the role of transition from SRC to RC. All specimens show similar discipline of stiffness degradation and the process can be divided into three parts. Some specimens of transfer column lose bearing capacity swiftly after shear cracking and showed weak energy dissipation ability, but the others show better ability of energy dissipation than RC column.

Keywords: steel reinforced concrete; hybrid structure; transfer column; displacement ductility; cyclic test; seismic behavior

1. Introduction

Steel reinforced concrete (SRC) structures were widely used in high-rise building for its good behavior to resist seismic motions and fire accident (Oyawa *et al.* 2007, Gonçalves and Carvalho 2004, Chen *et al.* 2006, Tikka and Mirza 2006, Chung *et al.* 2012, Du *et al.* 2013). Compared with reinforced concrete (RC) structures, the shape steel in SRC structures improves not only load bearing capacity and stiffness but also deformation ability and ductility (Chen *et al.* 2014, Rodrigues *et al.* 2015). However, massive shape steel configuration in SRC structure will push up the construction cost that is the reason for its limitation in multi-storey buildings (Bae and Bayrak 2008, Park *et al.* 2012, Yamashita and Sanders 2009, Pandey *et al.* 2008). In the economically underdeveloped areas, construction cost is an important factor for structure

*Corresponding author, Associate Professor, E-mail: Wukai19811240@163.com

^a Professor, E-mail: jianyang_xue@163.com

^b Postgraduate Student, E-mail: 514894557@qq.com

^c Professor, E-mail: zhaohongtie@hotmail.com

application. Even for high-rise buildings, SRC structures are mainly used at the developed area of China.

SRC-RC hybrid structure mixes the characteristic and benefit of SRC and RC structure. It sets SRC columns at bottom floors where suffer almost the whole self-weight structure and reinforced concrete (RC) columns at upper floors whose burden is relatively small, so SRC and RC structure show their benefits in a more economic way (Dai *et al.* 2003, Yang *et al.* 2006), while seismic resistance of the hybrid structure improves without significant raise of project cost.

SRC-RC hybrid structures were first promoted in Japan and widely used in some areas of China. The transfer mode shown in Fig. 1(a) once was mostly used. Unfortunately, the SRC-RC hybrid structures with this transfer mode suffered severe damage in Hyogoken-Nanbu earthquake of 1995, as shown in Fig. 2 (Azizinamini and Ghosh 1997). The failure mainly concentrated at the transfer stories, for the reason that sudden change of lateral stiffness. To avoid this disadvantage, a new transfer mode was brought forward, in which shape steel extends to the middle position of column in transfer story, as shown in Fig. 1(b). This transfer mode leads to the appearance of the SRC-RC transfer column as shown in Fig. 3, which has a partial shape steel in the column (Suzuki *et al.* 1999, Yamaguchi *et al.* 2004, Kon-No *et al.* 1998, Kimura and Shingu 1998). SRC-RC transfer columns used for linking the SRC columns below and the RC columns above and smoothing the sudden change of lateral stiffness and avoid seismic damage concentration.

Because of the practicability, some high-rising buildings and multi-storey buildings adopted transfer columns as structural transformation from SRC to RC. Nevertheless, the current seismic design criteria of China for the structural transformation still remain as the old transfer mode and cannot satisfy the new demand of seismic resistant design. Some scholars did a small number of experiments to explore the behavior of SRC-RC transfer column. Suzuki completed a pseudo-dynamic test of 5 specimens to evaluate the influence of shape steel extended length on cyclic performance of SRC-RC transfer column. Yamaguchi compared the skeleton curves of SRC column, RC column and SRC-RC transfer column based on a test of 3 specimens. Although these tests give us some primary understanding of SRC-RC transfer column, they are not enough to comprehensively estimate the seismic behavior due to the lack of systematical study. Some critical factors may be seriously affect the seismic behavior of SRC-RC transfer column, such as area ratio of shape steel and the volumetric ratio of lateral ties, but the researches on these factors still stay blank.

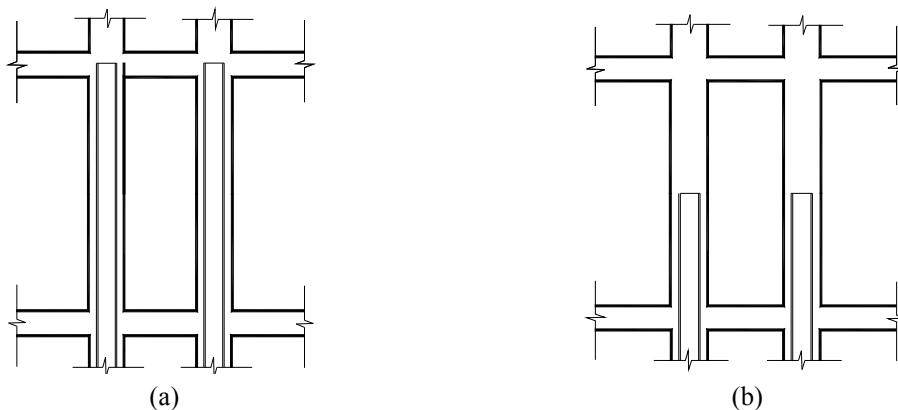


Fig. 1 Transfer modes of SRC-RC hybrid structures



Fig. 2 Damage of SRC-RC hybrid structures

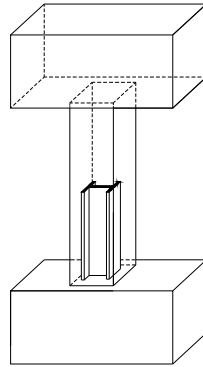


Fig. 3 SRC-RC transfer column

Based on the existing research, a pseudo-dynamic test of 17 specimens was finished to study the cyclic behavior of SRC-RC transfer column. The influence of 4 critical factors was analyzed, including axial compressive ratio, arrangement of lateral ties, extended length of shape steel and area ratio of shape steel, which are related to the seismic behavior. This paper focuses on the study of failure mode and hysteretic behavior of the transfer column. This research and the test are helpful of the national standard development and updating. Some instructive significances in practice have been obtained which can also play a directive role in seismic resistant design of structures.

2. Experimental program

2.1 Specimen design and materials

16 specimens of transfer column and 1 specimen of RC column are tested under low cyclic loading. All specimens have a section of 220 mm × 160 mm and a height of 1000 mm. The test parameters are the volumetric ratio ρ_{sv} of lateral ties, axial compressive ratio n , extended length L_{ss} and area ratio ρ_{ss} of shape steel. Two types of shape steel I10 and I14 are utilized here, whose

section properties are listed in Table 1. I is the moment of inertia, W is the elastic section modulus, i is the radius of gyration respect to the axis of bulking. Three models of lateral ties setting are adopted here, including normally setting as RC columns, double setting at the discontinuous location of shape steel and double setting all over the height of specimens. Each specimen is reinforced longitudinally with 4 deformed steel bars at each corner with diameter 16 mm.

All specimens were cast from one batch of concrete and the compressive strength is 59.1 Mpa, which was determined based on the average measurements of six 150 mm cubes. Two batches of steel were used and the properties are listed in Table 2. Steel skeletons of some specimens are shown in Figs. 4 and 5. The details for specimens are listed in Table 3.

Table 1 Section features of shape steel

Section parameters	I10	I14
h (mm)	100	140
b (mm)	68	80
d (mm)	4.5	5.5
t (mm)	7.6	9.1
r (mm)	6.5	7.5
r_1 (mm)	3.3	3.8
I_x (cm ⁴)	245.0	712.0
W_x (cm ³)	49	102.0
I_y (cm ⁴)	33.0	64.4
W_y (cm ³)	9.7	16.1
i_x (cm)	4.1	1.5
i_y (cm)	5.8	1.7

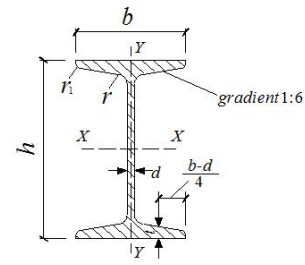


Table 2 Steel property

Batches	Types	Yield strength f_y /MPa	Ultimate strength f_u /MPa	Elastic modulus E_s /MPa
Batch 1	$\Phi 6.5$	364.3	461.5	2.01×10^5
	$\Phi 16$	376.0	547.4	1.91×10^5
	flange I10	267.6	428.1	1.85×10^5
	web I10	281.0	417.7	1.95×10^5
	flange I14	258.5	408.1	1.90×10^5
	web I14	300.4	432.7	2.03×10^5
Batch 2	$\Phi 6.5$	383.6	507.1	1.95×10^5
	$\Phi 16$	358.3	537.7	1.84×10^5
	flange I10	257.7	372.8	1.96×10^5
	web I10	296.1	388.5	2.04×10^5
	flange I14	292.7	433.1	2.04×10^5
	web I14	336.8	452.7	1.95×10^5



(a) Specimen SRC8-2 / SRC8-4



(b) Specimen S4-2-N



(c) Specimen S8-2/ S8-4



(d) Specimen S4-2 / S4-4

Fig. 4 Steel skeletons

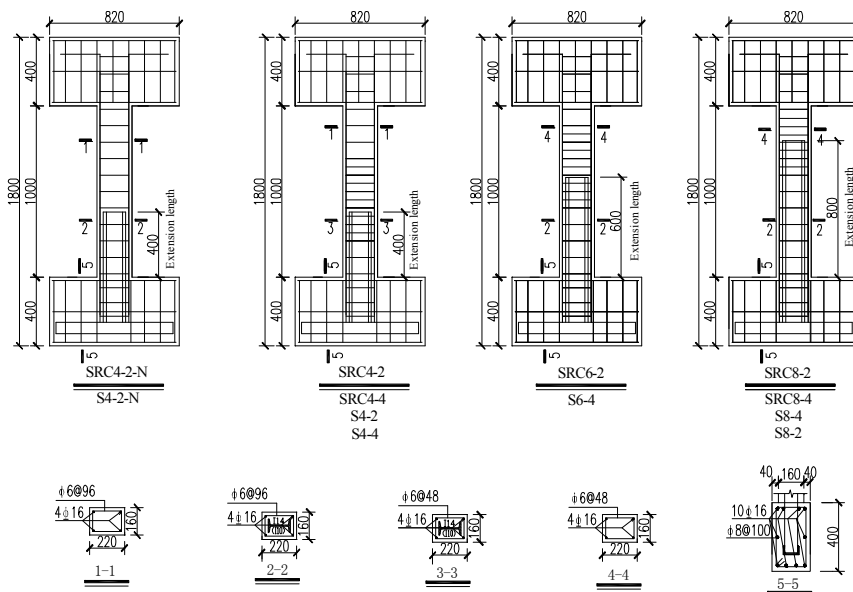
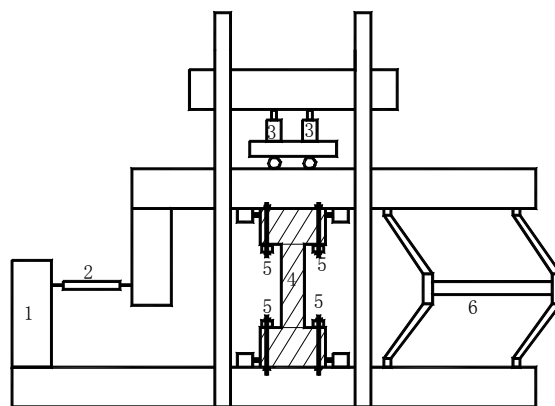


Fig. 5 Geometry and instrumentation of test specimens

Table 3 Properties of test specimens

Notation of specimens	Extended length of shape steel L_{ss}/mm	Axial compressive ratio n	Longitudinal reinforcement		Lateral ties		Lateral ties at location of shape steel discontinuous	Shape steel		Failure mode
			Setting	ρ_s /%	Setting	ρ_{sv} /%		Setting	ρ_{ss} /%	
SRC4-2-N*	400	0.2	4_16	2.28	6.5@96	0.96	-	I14	6.11	Shear
S4-2-N	400	0.2	4_16	2.28	6.5@96	0.96	-	I10	4.08	Shear
SRC4-2*	400	0.2	4_16	2.28	6.5@96	0.96	6.5@48	I14	6.11	Shear
SRC4-4	400	0.4	4_16	2.28	6.5@96	0.96	6.5@48	I14	6.11	Shear
S4-2*	400	0.2	4_16	2.28	6.5@96	0.96	6.5@48	I10	4.08	Shear
S4-4	400	0.4	4_16	2.28	6.5@96	0.96	6.5@48	I10	4.08	Shear
SRC6-2	600	0.2	4_16	2.28	6.5@96	0.96	6.5@48	I14	6.11	Shear
S6-4	600	0.4	4_16	2.28	6.5@96	0.96	6.5@48	I10	4.08	Bend
SRC8-2*	800	0.2	4_16	2.28	6.5@96	0.96	6.5@48	I14	6.11	Bond
SRC8-4	800	0.4	4_16	2.28	6.5@96	0.96	6.5@48	I14	6.11	Shear
S8-2*	800	0.2	4_16	2.28	6.5@96	0.96	6.5@48	I10	4.08	Bend
S8-4	800	0.4	4_16	2.28	6.5@96	0.96	6.5@48	I10	4.08	Bond
SRC4-2-JM*	400	0.2	4_16	2.28	6.5@96	1.92	-	I14	6.11	Shear
SRC4-4-JM	400	0.4	4_16	2.28	6.5@96	1.92	-	I14	6.11	Shear
S4-2-JM*	400	0.2	4_16	2.28	6.5@96	1.92	-	I10	4.08	Shear
S4-4-JM	400	0.4	4_16	2.28	6.5@96	1.92	-	I10	4.08	Shear
RC	-	0.2	4_16	2.28	6.5@96	0.96	-	-	-	Bend

Note: * means steel of batch 1.



1. Reaction steel wall 2. Actuator 3. Hydraulic jacks
4. Specimen 5. High-strength screws 6. Pantograph

Fig. 6 Overall view of test set-up

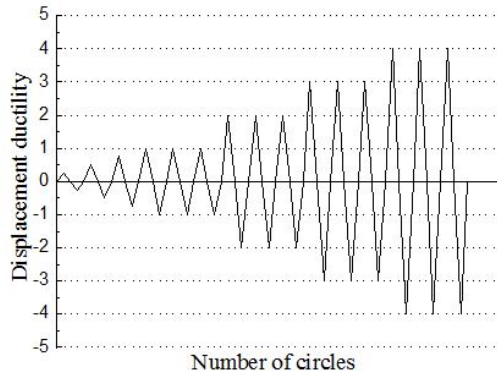


Fig. 7 Lateral displacement history

2.2 Testing procedure

Lateral load was applied by an MTS servo-controlled hydraulic actuator to top of the specimens. Axial load was exerted through two hydraulic jacks. Setup of loading apparatus is shown in Fig. 6. A test protocol was used to investigate the cyclic behavior of the specimens. The column was laterally subjected to a predetermined cyclic history as indicated in Fig. 7. Loading process of specimens is controlled by load at first and then controlled by displacement after yield condition.

3. Analysis, results and discussions

Analysis and discussion were carried out on failure modes, hysteretic loops, skeleton curves, characteristic values of load and displacement, stiffness degradation curves, and energy dissipation.

3.1 Failure modes

Failure of transfer columns can be roughly divided into three modes: shear failure, bond failure and bend failure. Transfer columns suffer shear effect seriously, which is mainly due to the partially existence of shape steel. Fig. 8 shows failure patterns of representative specimens. When lateral ties were normally set as RC columns, critical shear crack of transfer columns ran through the whole specimens, corresponding failure pattern is shown in Fig. 8(a).

If more lateral ties were set at the discontinuous location of shape steel, shear failure patterns changed to Figs. 8(b)-(c). Damage location shifts to top of the specimens, typical pattern of shear cracks is axial distribution and development from the top corners as starting points. Although lateral ties can effectively control the development of shear cracks, the tiny shear cracks divided concrete into several pieces. Integrity of concrete diminished, and hence specimens lost their bearing capacity under the interaction of axial force, bending moment and shear force. If crushed concrete was removed after experiment loading, the residual concrete at damage location was shaped as tension which is shown in Fig. 8(d).

Due to the adequate development of shear cracks during the loading period, shear failure engendered at top of specimens, but bend failure was always engendered at SRC section of column bottom, failure pattern is shown in Fig. 8(e). Bending strength of SRC cross section is related to

arrangement of shape steel, so diminishing the section of shape steel can be conducive to the emergence of bend failure. The only two specimens engendered bend failure are both arranged with shape steel of I10, area ratio of shape steel is 4.08%. Sufficient extended length of shape steel is also decisive to bend failure. As the shape steel partially existed in the lower part of specimens, the shear force beard by shape steel comes from concrete through interaction of two materials, and the interaction mainly took place at the discontinuous position of shape steel. Sufficient extended length of shape steel can provide more distance of shear force arm, so cross section of SRC can achieve flexural yield condition, which is the prerequisite for bend failure. Bend failure can only be achieved when extended length of shape steel is not less than triple of the long side of cross section. But bond cracks would be engendered and developed sufficiently when extended length kept increasing.

Bond failure occurred when extended length of shape steel achieves 800 mm particularly with higher axial compressive ratio and more shape steel. During the procedure of bond failure, shear cracks firstly appeared at middle part of specimens but steel web restricted the development of shear cracks. Then bond cracks emerged at the location of steel flanges, which ranged from bottom of columns to the discontinuous position of shape steel. While the bond cracks developed and connected with each other, bearing capacity of specimens degenerated rapidly with the increment of loading cycle, concrete cover of steel flanges was crushed in the end and loading procedure finished. Bond failure pattern is shown in Fig. 8(f).



(a) Specimen SRC4-2-N



(b) Specimen SRC4-4-JM



(c) Specimen S4-4



(d) Specimen SRC4-4



(e) Specimen S8-2



(f) Specimen S8-4

Fig. 8 Specimens after failure

3.2 Hysteresis loops

Fig. 9 shows hysteresis loops of transfer columns. Hysteresis loops are important foundation for the evaluation of seismic behavior, which can reflect not only failure mechanism but also the mechanical characteristics such as bearing capacity, stiffness, displacement ductility and energy dissipation ability. Some conclusions can be deduced from the hysteresis loops.

- (1) Before concrete cracking, area of hysteresis loops is limited, relationship between load and displacement is almost linear, and rigidity degradation and residual deformation are quite small. After cracking, area of hysteresis loops increases with the increment of load, and rigidity degradation becomes obvious. Specimens get into elastic-plastic stage. At the period of displacement control, specimens have reached plastic stage, and then bearing capacity degenerated more seriously at same increment of displacement, which is mainly due to the development of cracks and cumulative damage of concrete. At the same time, fold phenomenon engenders.
- (2) The partially existence of shape steel in transfer column not only changes failure mechanism but also leads to fold phenomenon in hysteresis loops. Fold phenomenon comes from the opening and closing of cracks, which is mainly effected by the amount of lateral ties, cross section of shape steel and axial compressive ratio. If more lateral ties are arranged, shear crack and bond crack can be controlled and hysteretic loop will be chubbiness.
- (3) Axial compressive ratio has serious effect on hysteresis loops and seismic behavior of transfer columns. Axial compressive force contributes to bearing capacity but restricts the deformation and deflection of specimens. Axial compressive force also accelerates the development of bond crack and leads to serious degradation of bearing capacity. Area of hysteresis loops will decrease and energy dissipation ability will degenerate if axial compressive ratio increased.
- (4) Extended length of shape steel influences the characteristic of hysteresis loops. Fold phenomenon of the specimens with extension coefficient $\zeta = 0.8$ is more obvious than that of 0.4. Bond cracks exist at the interface of concrete and steel flanges. If extended length of shape steel increased, more bond cracks will engendered and energy dissipation ability will degrade.

3.3 Skeleton curves and postpeak behavior

Fig. 10 shows the skeleton curves of transfer columns, which presents of postpeak behavior.

- (1) Extended length of shape steel has serious effect on the postpeak behavior of transfer column. Deformation ability of transfer column after yield condition will reach optimization if extended length of shape steel is 3/5 of the column height.
- (2) Axial force influences the bond performance between concrete and shape steel, leads to much more bond cracks and hence deteriorates the postpeak behavior of transfer column.
- (3) Area ratio of shape steel has negative effect on postpeak behavior of transfer column, skeleton curves will drop swiftly after peak point if more shape steel was deposited, and the effect has relationship with arrangement of lateral ties and can be weakened by increment of lateral ties.
- (4) Arrangement of lateral ties is the most important factor for postpeak behavior of transfer

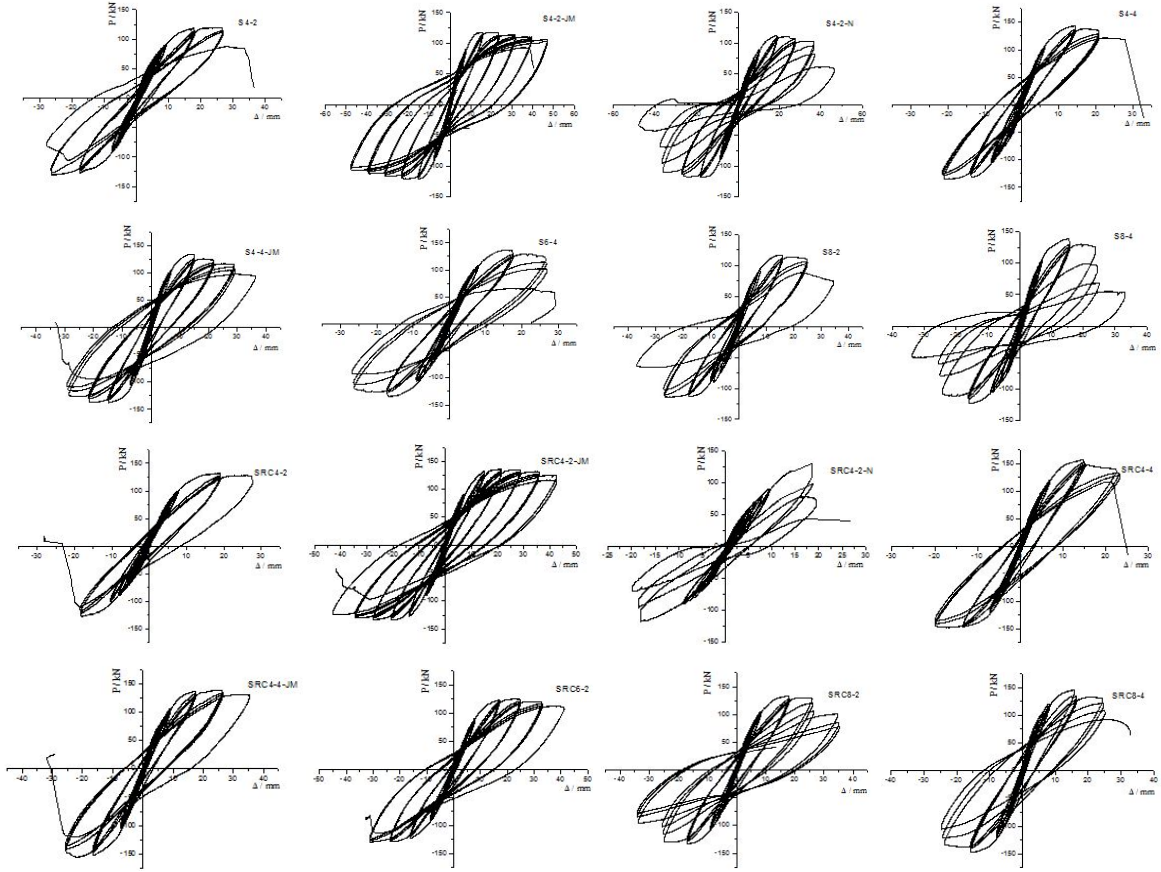


Fig. 9 Hysteresis loops of SRC-RC specimens

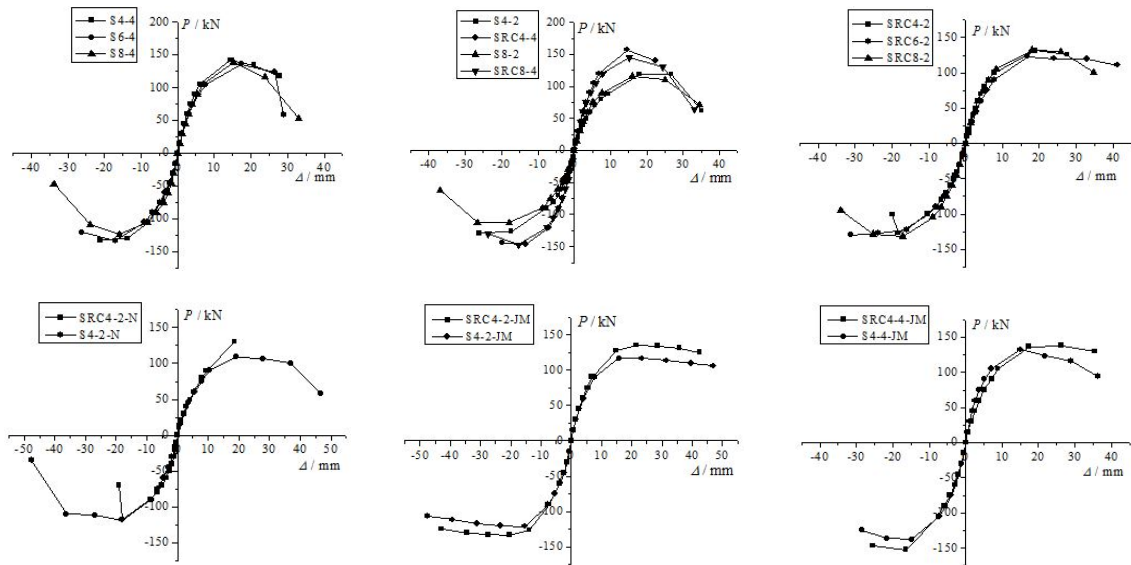


Fig. 10 Skeleton curves

column. Load degradation after peak point will slow down and lowest residual capacities will be better if more lateral ties are arranged.

3.4 Characteristic value of load and displacement

Some characteristic values of load and displacement can be obtained from hysteresis loops and skeleton curves. Characteristic values of 16 transfer columns and 1 RC column are all listed in Table 4, including cracking load P_{cr} , yield load P_y , maximum load P_m , and the corresponding displacement Δ_{cr} , Δ_y , Δ_m . Ultimate displacement Δ_u here is used to calculate the displacement ductility coefficient μ . Δ_u is defined as the displacement of failure or bearing capacity degenerated to $0.85P_m$, μ can be calculated as $\mu = \Delta_u/\Delta_y$. Due to the asymmetry of hysteresis loops, displacement ductility coefficients at direction of pull and push are different, and hence μ can be calculated by the formula below

$$\mu = \frac{|\Delta_{+u}| + |\Delta_{-u}|}{|\Delta_{+y}| + |\Delta_{-y}|} \quad (1)$$

Displacement ductility coefficient of RC column is 4.19, and the values of transfer columns change from 1.97 to 5.99. Seismic behavior of transfer columns was quite different. Because of the partially existed shape steel, shear stress in transfer columns is bigger than RC columns, and hence 12 of the 16 transfer columns failed in shear. Extension ratio, axial compressive ratio, cross section of shape steel and volumetric ratio of lateral ties show different effects on displacement ability and seismic behavior of transfer columns. Coupling of the 4 factors leads to the diversity of displacement ductility coefficients in transfer columns.

Partially existed shape steel makes the abnormal change of internal stress passing and hence leads to serious shear effect to transfer columns. Therefore, displacement ductility decreases along with the section increment of shape steel. All the 8 specimens with shape steel of I10 satisfied seismic requirement of displacement ductility, but 3 specimens in 8 with shape steel of I14 failed to satisfy the requirement.

The test results show similar trend with previously researches that displacement ductility is serious affect by extended length of shape steel. As the extended length of shape steel increasing, displacement ductility improves at first and then reduces, and reaches peak point when length of shape steel is about 3/5 height of column, shown in Fig. 11. Especially for the specimens with low level of axial compression, the effect is obvious. Hence for seismic resistant design, SRC-RC transfer column will be at top performance if shape steel extended length gets to 3/5 height of the column.

Transfer columns suffer serious shear effect and lateral ties show great effect on seismic behavior. Displacement ductility improves rapidly with increment of lateral ties. The lateral ties provide lateral restriction to concrete inside and make core concrete under three-dimensional compression, which upgrades strength as well as ultimate strain of concrete. What is more, lateral ties restrict cracks and maintain the integrality of concrete. Therefore, the arrangement of lateral ties for SRC-RC transfer column should not less than the double of RC column to satisfied the seismic resistant demand.

Displacement ductility of transfer columns decreases with the improvement of axial compressive ratio, which is same as that of RC columns and SRC columns. Rotation ability of plastic hinge leads to lateral displacement of specimens and makes advanced ductility and

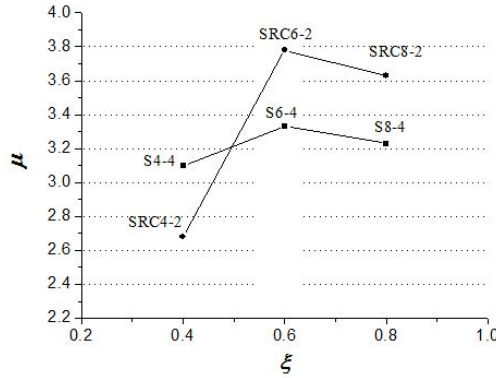


Fig. 11 Relationship between displacement ductility and extended length of shape steel

postpeak behavior. Axial compression limits the rotation ability of cross section and makes the characteristic of plastic hinge from tension to compression, and hence displacement ductility decreases. On the other hand, axial compression effects the development of cracks. For specimens with short length of shape steel, shear crack ultimately leads to failure. Axial compression improves shear strength of concrete and limits the development of shear cracks, and restriction of lateral ties will be weakened. Displacement ductility of the specimens with more lateral ties is more effected by axial compressive ratio, illuminated in Fig. 12. For specimens with long length of shape steel, bond crack is a big problem, which leads to seismic behavior degradation. The development of bond cracks is closely related to axial compression, specimens suffer serious effect of bond cracks and show degradation of ductility under compression of $n = 0.4$.

3.5 Stiffness and degradation behavior

Stiffness of transfer column is presented by the secant at characteristic points of skeleton curves. Table5 gives D_c , D_y , D_m , which respectively present the stiffness of cracking point, yield point and peak point of bearing capacity. D_c changes from 14.42 kN/mm to 25.92 kN/mm; D_y changes from 9.91 kN/mm to 16.64 kN/mm; D_m changes from 4.89 kN/mm to 9.68 kN/mm. The stiffness of transfer columns is at the interval of SRC and RC columns, and hence transfer columns can play the role of transition element from SRC column to RC column.

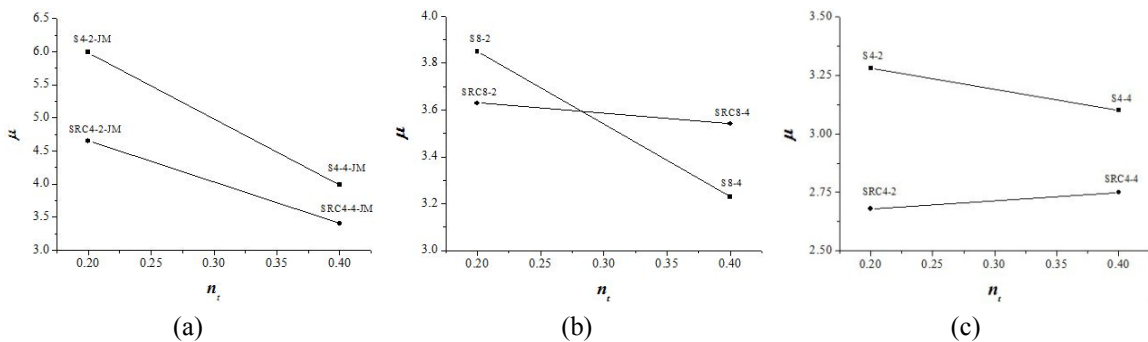


Fig. 12 Axial compressive ratio and displacement ductility

Table 4 Characteristic value of load and displacement

Notation of specimens	Characteristic displacement / mm								Characteristic load /kN						Displacement ductility μ
	Push(+)				Pull(-)				Push(+)			Pull(-)			
	Δ_{cr}	Δ_y	Δ_m	Δ_u	Δ_{cr}	Δ_y	Δ_m	Δ_u	P_{cr}	P_y	P_m	P_{cr}	P_y	P_m	
SRC4-2-N	2.40	10.74	18.57	18.57	1.47	8.02	17.96	18.35	35	98.7	130.1	35	85.3	117.8	1.97
S4-2-N	2.12	8.99	18.33	37.91	1.80	8.79	18.01	37.59	30	83.1	112.4	30	90.7	118.6	4.24
SRC4-2	2.02	8.19	18.68	27.58	1.56	9.34	18.06	19.42	40	103.4	132.3	30	97.3	127.5	2.68
SRC4-4	1.88	8.08	14.58	22.41	1.98	7.27	17.18	19.79	50	130.9	157.0	50	124.2	147.5	2.75
S4-2	2.03	8.67	25.28	29.35	2.14	8.26	25.90	26.20	35	88.9	120.1	40	97.2	130.2	3.28
S4-4	2.92	7.18	14.40	26.13	2.48	8.04	19.95	21.11	65	115.9	143.2	50	105.0	134.8	3.10
SRC6-2	1.70	9.22	23.06	41.19	3.89	9.92	31.04	31.21	25	99.1	125.6	55	100.0	129.7	3.78
S6-4	2.24	7.68	15.42	26.74	3.50	8.18	16.72	26.09	50	105.0	136.9	60	100.7	134.7	3.33
SRC8-2	1.34	8.17	17.77	31.06	2.49	8.37	17.03	29.07	30	105.0	133.0	45	103.6	133.4	3.63
SRC8-4	3.25	6.91	14.92	25.29	3.34	6.96	15.30	23.75	75	112.2	145.1	75	115.2	147.4	3.54
S8-2	1.69	7.02	15.12	27.68	1.68	7.93	24.28	29.88	35	85.5	116.3	30	84.7	113.9	3.85
S8-4	1.67	7.89	15.43	22.55	2.18	6.73	15.88	24.65	35	114.5	139.6	55	95.6	123.8	3.23
SRC4-2-JM	1.77	9.17	21.33	42.4	2.03	9.15	19.48	42.9	35	103.4	135.7	40	100.7	133.7	4.65
SRC4-4-JM	2.21	8.87	26.22	35.37	2.29	9.09	21.97	25.45	40	105.0	139.2	50	124.5	155.5	3.39
S4-2-JM	1.87	7.91	19.33	46.99	3.13	7.89	15.29	47.62	35	88.7	118.1	55	92.0	121.1	5.99
S4-4-JM	3.81	6.86	14.21	29.46	2.83	7.72	14.75	28.51	75	105.0	134.2	60	115.9	137.9	3.98
RC	0.83	8.44	23.62	32.11	0.69	6.55	15.20	30.74	15	73.7	100.2	15	82.0	103.6	4.19

Shape steel strengthens cross sections and improves the capacity and stiffness. Hence cracking loads of transfer columns are higher than those of RC columns. Average lateral stiffness of 16 transfer columns and that of RC have only the difference in the rate of 0.5% at the point of concrete cracking. When specimens reached the condition of yielding, the rate of differences rises up to 15.9%. At last, when loads raise up to bearing capacity, the rate gets to the point of 24.7%. While the damage of concrete increasing with load increment, shape steel plays a more important role in load resistance and has more interaction with concrete, strengthening effect of shape steel was more obvious. So, the lateral stiffness differences of transfer columns and RC columns become more obvious.

Coefficient η is defined as the ratio of lateral stiffness D of different drift angle θ to elastic lateral stiffness D_0 , which can reflect the degradation of lateral stiffness. The stiffness at peak point of the first cyclic loading is adopted as D_0 . Figs. 13(a) and (b) give the relation between lateral stiffness degradation and drift angle θ .

All specimens of transfer columns show similar pattern of degradation. The degradation rate is swift at the period from concrete cracking to yield condition but slow down later.

According to damage and mechanical performance, the process of stiffness degradation can be divided into three parts.

- (1) First stage is from test beginning to concrete cracking. Concrete and steel stay in the

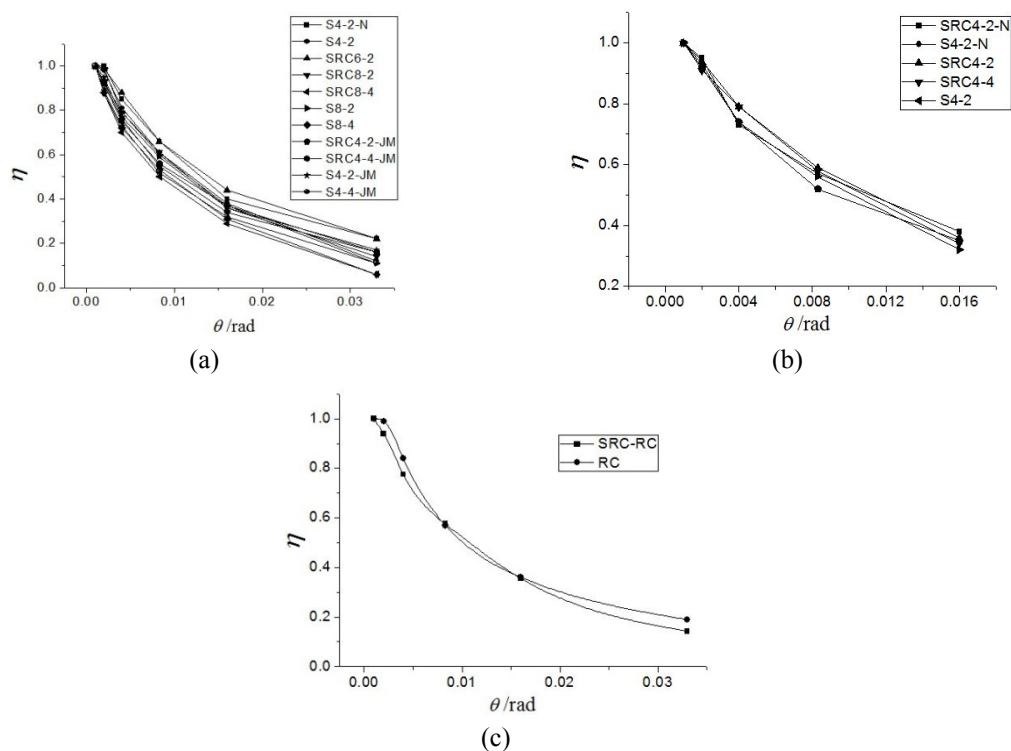


Fig. 13 Stiffness degradation ratio

condition of elasticity. However, stiffness has small reduction, which is mainly due to the tiny cracks and nonlinear performance of concrete. Hysteresis loops are almost linear at this period, while loading curves and unloading curves are almost superposed. Stiffness has good stability.

- (1) Second stage is from the first crack to yield. Cracks of bond, shear and bend emerge one by one at this stage and lead to acceleration of stiffness degradation. Due to the development of bond cracks, interactions between both materials become weak, which also lead to the degradation of stiffness. Specimens have obvious nonlinear characteristic and hysteresis loops turn to curve at this stage.
- (2) Third stage is from yield condition to ultimate condition. When load decreases to 0.85 of bearing capacity, specimens reach the ultimate condition. A majority of cracks appear at second stage but a few at this stage, so stiffness degradation slows down. However, cracks extended and slip between concrete and steel engendered with development of bond cracks. Hence hysteresis loops show obvious fold phenomenon at this stage, which will be much more serious if extended length of shape steel increases.

Fig. 13(c) shows the average stiffness degradation curves of the 16 transfer columns, which are compared with that of RC column. Although stiffness of transfer columns is higher than that of RC column, they both share similar rule of stiffness degradation. Stiffness degradation can be neglected if lateral drift angle is no larger than $1/550$. Otherwise, coefficient η is used for express the stiffness degradation during the cyclic loading and can be calculated by the formula below. The

calculated results are consistent with the test results of this paper and previously researches.

$$\eta = \frac{D}{D_0} = e^{-60\theta} \tag{2}$$

Although 16 specimens of transfer column share similar rule of stiffness degradation, axial force, configuration and steel arrangement have great effect on the rate of stiffness degradation. Bond cracks contribute much to the stiffness degradation, and hence specimens with high level of axial compression and longer extension of shape steel suffers high rate of stiffness degradation, such as specimen SRC8-4. Eq. (3) is for upper limit of degradation curves; and Eq. (4) is for lower limit of degradation curves.

$$\eta = \frac{D}{D_0} = e^{-48\theta} \tag{3}$$

$$\eta = \frac{D}{D_0} = e^{-86\theta} \tag{4}$$

3.6 Energy dissipation

Energy dissipation can be presented by h_e , which is expressed as

Table 5 Stiffness of specimens

Notation of specimens	D_c /(kN/mm)			D_y /(kN/mm)			D_m /(kN/mm)		
	Push(+)	Pull(-)	Average	Push(+)	Pull(-)	Average	Push(+)	Pull(-)	Average
SRC4-2-N	14.58	23.81	19.20	9.19	10.64	9.91	7.01	6.56	6.78
S4-2-N	14.15	16.67	15.41	9.24	10.32	9.78	6.13	6.59	6.36
SRC4-2	19.80	19.23	19.52	12.63	10.42	11.52	7.08	7.06	7.07
SRC4-4	26.60	25.25	25.92	16.20	17.08	16.64	10.77	8.59	9.68
S4-2	17.24	18.69	17.97	10.25	11.77	11.01	4.75	5.03	4.89
S4-4	22.26	20.16	21.21	16.14	13.06	14.60	9.94	6.76	8.35
SRC6-2	14.71	14.14	14.42	10.75	10.08	10.41	5.45	4.18	4.81
S6-4	22.32	17.14	19.73	13.67	12.31	12.99	8.88	8.06	8.47
SRC8-2	22.39	18.07	20.23	12.85	12.38	12.61	7.48	7.83	7.66
SRC8-4	23.08	22.46	22.77	16.24	16.55	16.39	9.73	9.63	9.68
S8-2	20.71	17.86	19.28	12.18	10.68	11.43	7.69	4.69	6.19
S8-4	20.96	25.23	23.09	14.51	14.21	14.36	9.05	7.80	8.42
SRC4-2-JM	19.77	19.70	19.74	11.28	11.01	11.14	6.36	6.86	6.61
SRC4-4-JM	18.10	21.83	19.97	11.84	13.70	12.77	5.31	7.08	6.19
S4-2-JM	18.72	17.57	18.14	11.21	11.66	11.44	6.11	7.92	7.01
S4-4-JM	19.69	21.20	20.44	15.31	15.01	15.16	9.44	9.35	9.40
RC	18.07	21.74	19.91	8.73	12.52	10.63	4.24	6.82	5.53

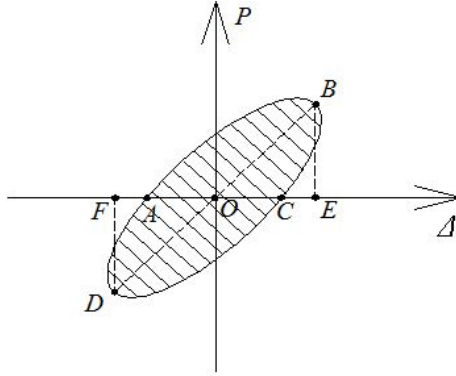


Fig. 14 Hysteretic loop

$$h_e = \frac{S_{(ABC+CDA)}}{2\pi \cdot S_{(OBE+ODF)}} \quad (5)$$

Where $S_{(ABC+CDA)}$ is area of the hysteresis loop and $S_{(OBE+ODF)}$ is area of triangles corresponding to peak points of the hysteresis loop, as shown in Fig. 14.

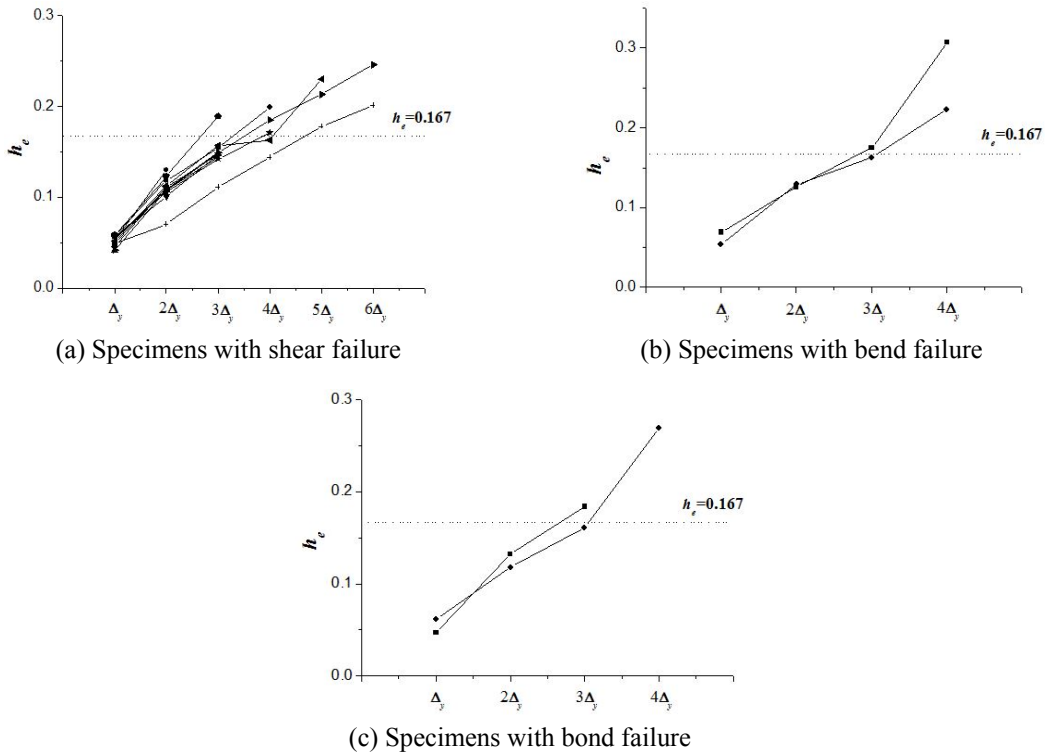


Fig. 15 Curves of energy dissipation

Fig. 15 shows the variation of h_e during the loading period of displacement control, h_e here is from the first cycle of loading. Half of the 12 specimens with shear failure have better energy dissipation ability than RC column, 4 specimens with bend failure or bond failure all show advanced energy dissipation ability. h_e of transfer columns can reach up to 0.307, which is much higher than 0.167 of RC column. Energy dissipation behavior of transfer columns is at the interval of RC columns and SRC columns.

Plastic deformation and concrete damage are the main manners for energy dissipation. Some specimens lose bearing capacity swiftly after shear cracking which is mainly due to weak configuration of those specimens. Hence, the development of plastic performance and deformation ability of cross section has little contribution to energy dissipation ability. The others show better ability of energy dissipation than RC column, which can be explained as below:

- (1) Shear span of RC column is 2.5 and its failure is bend mode, the dissipated energy is mainly from the both ends of the column where the damage are focused on. For transfer columns, energy dissipation ability comes from not only the cumulative damage from bend deformation at both ends but also bond cracks and shear cracks along the height of columns.
- (2) Shape steel in transfer columns prolongs the failure process of cross sections, so specimens show better ductility and deformation ability. Due to the reinforcement effect of shape steel, ultimate rotated angle and plastic development of transfer columns promote, more area reaches yield condition and contributes to the deformation ability.

4. Conclusions

In this work, a pseudo-dynamic test of 17 specimens was conducted to research the seismic behavior of transfer columns in SRC-RC hybrid structures. The following conclusions were drawn from the results of this research.

- (1) Failure of transfer columns can be roughly divided into shear failure, bond failure and bend failure. Partially existed shape steel makes the abnormal change of internal stress passing and leads to serious shear effect to transfer columns, most specimens engendered shear failure.
- (2) Displacement ductility coefficient of transfer columns changes from 1.97 to 5.99, coupling of seismic design parameters leads to the diversity of displacement ductility coefficients. Displacement ductility of transfer column is serious affect by extended length of shape steel. As the extended length of shape steel increasing, displacement ductility improves at first and then reduces. The changed trend is similar with previously researches and the seismic behavior will be at top performance if shape steel extended length gets to 3/5 height of the column.
- (3) For specimens with long length of shape steel, bond crack is a big problem, which leads to seismic behavior degradation. The development of bond cracks is closely related to axial compressive level.
- (4) Stiffness of transfer columns is higher than that of RC column, and they both share similar rule of stiffness degradation. A coefficient have been deduced to express the degradation trend during cyclic loading period, which is consistent with the test results of this paper and Japanese references.
- (5) Energy dissipation behavior of transfer columns is at the interval of RC columns and SRC

columns. Half of the 12 specimens with shear failure have better energy dissipation ability than RC column, 4 specimens with bend failure or bond failure all show advanced energy dissipation ability. h_e of transfer columns can reach up to 0.307, which is much higher than 0.167 of RC column.

Acknowledgments

This work is supported by National Natural Science Foundation of China (Grant No.51208175; 50978217), Postdoctoral Science Foundation of China (Grant No.2012M511186) and the Fundamental Research Funds for the Central Universities (Grant No.2015B17514).

References

- Azizinamini, A. and Ghosh, S.K. (1997), "Steel reinforced concrete structures in 1995 Hyogoken-Nanbu earthquake", *J. Struct. Eng.*, **123**(8), 113-138.
- Bae, S.J. and Bayrak, O. (2008), "Seismic performance of full-scale reinforced concrete columns", *ACI Struct. J.*, **105**(2), 123-133.
- Chen, C.C. and Lin, N.J. (2006), "Analytical model for predicting axial capacity and behavior of concrete encased steel composite stub columns", *J. Construct. Steel Res.*, **62**(5), 424-433.
- Chen, C., Wang, C. and Sun, H. (2014), "Experimental study on seismic behavior of full encased steel-concrete composite columns", *J. Struct. Eng.*, **140**(6), 04014024.
- Chung, Y.S., Shim, C.S. and Hong, H.K. (2012), "Shake table tests of steel embedded composite columns under moderate near-fault motion", *Steel Structure*, **12**(4), 551-562.
- Dai, G.L., Jiang, Y.S., Fu, C.G. and Shuting, L. (2003), "Experimental study on aseismic behaviors of transfer story with steel reinforced concrete in low stories of large space", *China Civil Eng. J.*, **36**(4), 24-32.
- Du, E.F., Shu, G.P. and Mao, X.Y. (2013), "Experimental study on aseismic behaviors of transfer story with steel reinforced concrete in low stories of large space", *Steel Structure*, **13**(1), 129-140.
- Gonçalves, R. and Carvalho, J. (2014), "An efficient geometrically exact beam element for composite columns and its application to concrete encased steel I-sections", *Eng. Struct.*, **75**(5), 13-224.
- Guo, Z.H. (2013), *Reinforced Concrete Theory and Analyze*, Tsinghua University, Beijing, China.
- Kimura, J. and Shingu, Y. (1998), "Structural performance of SRC-RC mixed member under cyclic bending moment and shear", *Summaries of Technical Papers of Annual Meeting*, Architectural Institute of Japan, Kyushu, Japan, July.
- Kon-No, S., Imaizumi, T., Yamamoto, K. and Minami, K. (1998), "Experimental study on high-rise building with lower layer composed of SRC structure. Part 1: Outline of the tests about deformation capacity of SRC columns", *Summaries of Technical Papers of Annual Meeting*, Architectural Institute of Japan, Kyushu, Japan, July.
- Oyawa, W.O. (2007), "Steel encased polymer concrete under axial compressive loading: Analytical formulations", *Construct. Build. Mater.*, **21**(1), 57-65.
- Pandey, G.R., Mutsuyoshi, H. and Maki, T. (2008), "Seismic performance of bond controlled RC columns", *Eng. Struct.*, **30**(9), 2538-2547.
- Park, K.D., Kim, H.J. and Hwang, W.S. (2012), "Experimental and numerical studies on the confined effect of steel composite circular columns subjected to axial load", *Steel Structure*, **12**(2), 253-265.
- Rodrigues, J.P.C., Correia, A.J.M. and Pires, T.A.C. (2015), "Behaviour of composite columns made of totally encased steel sections in fire", *J. Construct. Steel Res.*, **105**(5), 98-106.
- Suzuki, H., Nishihara, H. and Matsuzaki, Y. (1999), "Shear performance of the column where structural form changes from SRC to RC", *Summaries of Technical Papers of Annual Meeting*, Architectural

- Institute of Japan, Chyugoku, Japan, July.
- Tikka, T.K. and Mirza, S.A. (2006), "Nonlinear equation for flexural stiffness of slender composite columns in major axis bending", *J. Struct. Eng.*, **132**(3), 387-399.
- Yamaguchi, M., Kimura, J., Chung, J. and Kawano, A. (2004), "Skeleton curve model of SRC-RC mixed columns", *Summaries of Technical Papers of Annual Meeting*, Architectural Institute of Japan, Hokkaidou, Japan, July.
- Yamashita, R. and Sanders, D.H. (2009), "Seismic performance of precast unbonded prestressed concrete columns", *ACI Struct. J.*, **106**(6), 821-830.
- Yang, Y., Zhang, Z. and Nie, Z. (2006), "Design of transition story of steel reinforced concrete (SRC) vertical hybrid structures", *J. Fuzhou Univ. (Natural Science)*, **34**(3), 399-404.

CC